VTT TIEDOTTEITA – MEDDELANDEN – RESEARCH NOTES 1778

Long-term behaviour of composite slabs prestressed with unbonded tendons

Mikko Malaska
Ecole polytechnique fédérale de Lausanne (EPFL)

Matti Pajari
VTT Building Technology

TECHNICAL RESEARCH CENTRE OF FINLAND
ESPOO 1996

ISBN 951–38–4973–2
ISSN 1235–0605

JULKAISIJA – UTGIVARE – PUBLISHER

Valtion teknillinen tutkimuskeskus (VTT), Vuorimiehentie 5, PL 2000, 02044 VTT
puh. vaihde (09) 4561, faksi (09) 456 4374

Statens tekniska forskningscentral (VTT), Bergsmansvägen 5, PB 2000, 02044 VTT
tel. växel (09) 4561, fax (09) 456 4374

Technical Research Centre of Finland (VTT), Vuorimiehentie 5, P.O.Box 2000, FIN–02044 VTT, Finland
phone internat. + 358 9 4561, fax + 358 9 456 4374

VTT Rakennustekniikka, Rakennusmateriaalit ja -tuotteet sekä puutekniikka, Kemistintie 3, PL 1805, 02044 VTT
puh. vaihde (09) 4561, faksi (09) 456 7004

VTT Byggnadsteknik, Byggnadsmaterial och -produkter, träteknik, Kemistvägen 3, PB 1805, 02044 VTT
tel. växel (09) 4561, fax (09) 456 7004

VTT Building Technology, Building Materials and Products, Wood Technology, Kemistintie 3, P.O.Box 1805, FIN–02044 VTT, Finland
phone internat. + 358 9 4561, fax + 358 9 456 7004

Technical editing Kerttu Tirronen

VTT OFFSETPAINO, ESPOO 1996

Malaska, Mikko & Pajari, Matti. Long-term behaviour of composite slabs prestressed with ubonded tendons. Espoo 1996, Technical Research Centre of Finland, VTT Tiedotteita – Meddelanden – Research Notes 1778. 29 p. + app. 11 p.

UDC 691:69.012.4:624.073
Keywords concrete construction, concrete slabs, slabs, steels, prestressing steels, steel construction, composite structures, finite element analysis, creep properties, shrinkage, relaxation (mechanics), tendons, unbonded tendons, strains, stresses

ABSTRACT

Mechanical modelling of post-tensioned steel-concrete composite slabs with unbonded tendons is discussed. The model was added as an option to COMPCAL, a finite element program developed at Ecole polytechnique fédérale de Lausanne, Switzerland. The work focused on the long-term behaviour of composite slabs in the serviceability limit state. Therefore, special attention was paid to the effects of creep and shrinkage of the concrete, and to those of relaxation of the prestressing steel. As an example, an analysis for a two-span slab was carried out.

PREFACE

In 1995-1996 a project entitled *Prestressing Techniques in Composite Floors* was carried out at VTT Building Technology. This report documents the work done in a subproject in which the COMPCAL computer program was modified into a form capable of analysis of post-tensioned composite slabs.

Mikko Malaska has done the programming work under the guidance of Matti Pajari and Antti Helenius, both from VTT. This report, written by Matti Pajari, is based on Mikko Malaska's Master's Thesis.

Rautaruukki Oy, the Technology Development Centre of Finland and VTT financed the project. Ecole polytechnique fédérale de Lausanne is acknowledged for permitting use of the COMPCAL program.

CONTENTS

LIST OF SYMBOLS

A	area of cross-section
A_{ps}	area of tendon cross-section
E	elasticity modulus
E_c	elasticity modulus of concrete
E_i	elasticity modulus of component i in composite cross-section
$E_{c,e}$	effective elasticity modulus of concrete
E_{c28}	elasticity modulus of concrete at the age of 28 days
$\overline{E}_{c,e}$	age-adjusted effective elasticity modulus of concrete
E^*	secant modulus
E_e^*	effective secant modulus
$\overline{E}_{c,e}^*$	age-adjusted effective secant modulus of concrete
J	creep function
L	length, span length
M	bending moment
M_c	bending moment restraining curvature due to free shrinkage, free creep or relaxation of prestressing steel
M_j	nodal bending moment at node j
N	normal force
N_c	normal force restraining axial strain due to free shrinkage, free creep or relaxation of prestressing steel
N_j	nodal force at node j
P	prestressing force
V	vertical force, shear force
h	drape of tendon, depth of cross-section
m	number of components of composite cross-section
t	time
t_0	time at loading
w	vertical uniformly distributed line load due to prestressing force
x	horizontal coordinate
y	vertical distance, positive direction downwards
y_{ps}	distance of tendon from reference plane, positive downwards
e	distance of tendon from reference plane, positive downwards

χ	aging coefficient
ε	strain
ε_0	strain at depth of reference plane
$\varepsilon_{c,e}$	instantaneous elastic strain of concrete
$\varepsilon_{c,c}$	strain of concrete due to creep
$\varepsilon_{c,sh}$	strain of concrete due to free shrinkage
$\varepsilon_{c,T}$	strain of concrete due to temperature change
$\varepsilon_{c,n}$	stress-independent component of concrete strain
$e_{c,\sigma}$	stress-dependent component of concrete strain
ε^k	strain at increment k
κ	curvature of beam or slab
σ	normal stress
σ_c	normal stress of concrete
σ_{p0}	initial prestress in tendon
σ_{pr}	prestress
σ^k	normal stress at increment k
θ	angle between tendon and horizontal plane
φ	creep coefficient

1 INTRODUCTION

The work described in this report, and also in Malaska's Diploma Thesis [8], is part of the project *Prestressing techniques in composite steel-concrete floors*. The aim has been to develop a finite element program for nonlinear analysis of post-tensioned steel-concrete composite slabs. The main concern has been the long-term behaviour of composite slabs prestressed with unbonded tendons.

A nonlinear finite element program entitled COMPCAL and developed at Ecole polytechnique fédérale de Lausanne (EPFL) has been used as the starting point. COMPCAL is based on the doctoral thesis of Byron J. Daniels. The theoretical background and architecture of the program are presented in publications of EPFL [4,5]. COMPCAL takes into account the nonlinear stress-strain relationship of the steel and concrete, the cracking of the concrete and the bond-slip at the interface of the concrete and the steel sheeting.

This study deals with post-tensioning with unbonded tendons. The forces due to the tensioning are modelled as transverse and axial loads calculated using the load-balancing method [7]. The deformations and inner forces due to the creep and shrinkage of the concrete, and those due to the relaxation of the prestressing steel, are calculated according to the recommendations of CEB-FIP Model Code 1990 [3] and Eurocode 2 [6].

The names of added and changed program modules are specified in Appendix F.

2 MODELLING TENDONS

The slab is modelled as a strip 1.0 m in width. The strip can be regarded as a post-tensioned beam. In the longitudinal direction, the total length of the slab is divided into n finite elements joined with n-1 nodes.

The tendon profile is modelled using six geometry types. The slab is divided into geometry fields, the end points of which coincide with nodes of the FEM model, in such a way that the whole tendon can be modelled using these geometry types (Fig. 1). The geometry in one field may consist of a straight line, a parabola or a combination of these. In the case of a multi-geometry field, the end points of each single geometric curve must coincide with nodes of the FEM model. The slope of the tendon is equal on both sides of a node jointing two adjacent geometry fields or two different curves within a field.

The properties of the geometry types used in the program are presented in Table 1. The formulae for determining the vertical loads due to the tensioning are derived by Tossavainen [9].

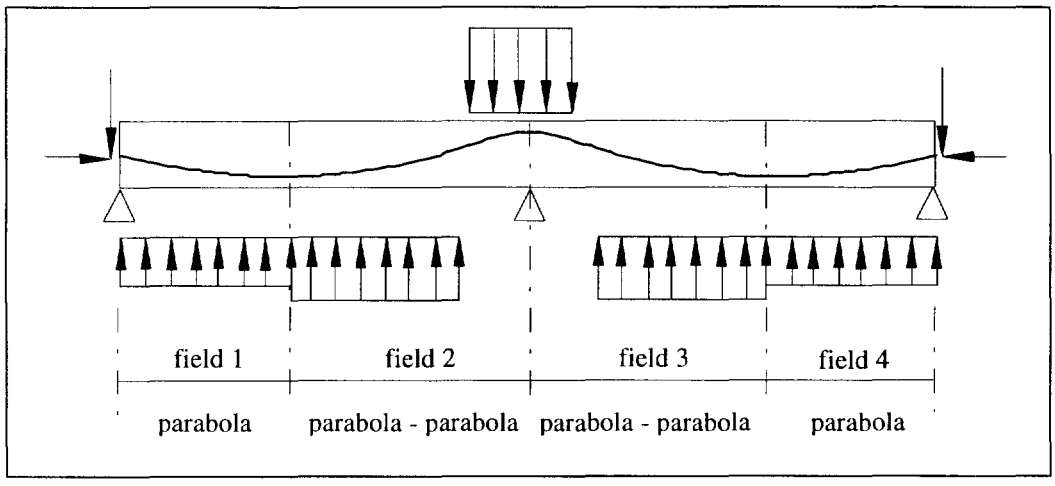

Fig. 1. Forces induced by a parabolic tendon.

Since the friction between the unbonded strands and ducts is small, it is ignored. This makes the tendon force constant over its whole length and makes it possible to model the horizontal forces due to post-tensioning as axial loads localized at the anchors.

The reaction forces caused by the anchors of the tendons are illustrated in Fig. 2.

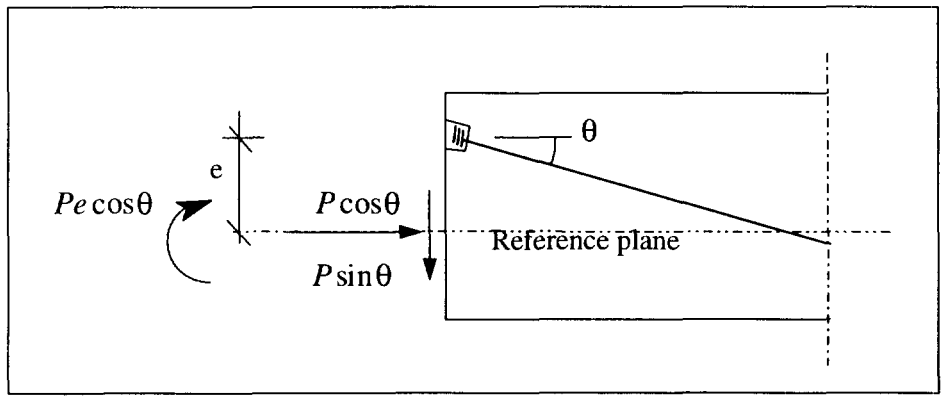

Fig. 2. Forces due to anchorage.

The program requires the following data about tendons:

- Title
- Cross-sectional area
- Initial stress σ_{p0}, i.e. stress in the tendon just after prestressing
- Number of geometry fields
- Tendon geometry in each field
  - Index of the first and last node
  - Geometry type
  - Index of nodes connecting different geometry in multi-geometry fields
  - Distance of tendon from bottom fibre of the composite slab at the aforementioned nodes.

Based on this information, the geometry of the tendons is calculated at the nodes and the vertical and axial forces are transformed into nodal forces. Thereafter, the tendon forces are treated as an external loading case.

Table 1 shows the geometry types, vertical forces and geometric parameters.

Table 1. Vertical forces due to tendon geometry (h/L_1 and $h/L_2 << 1$).

Type	Tendon geometry	Forces	
A	straight	$V = P(h / L_1)$	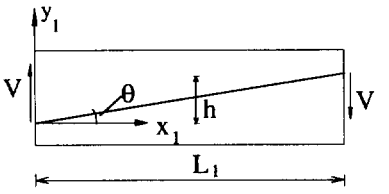
B	parabola	$w_b = \frac{2hP}{L_1^2}$	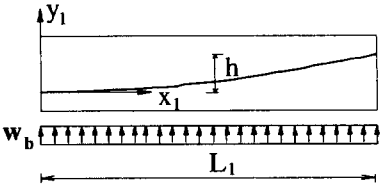
C	straight + parabola	$w_b = 2bP$ $b = \frac{h}{L_2(2L_1 + L_2)}$	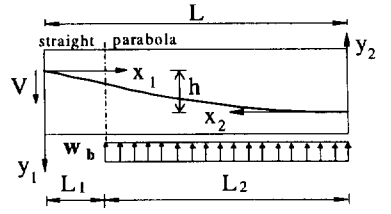

Continued

Table 1. Continued.

D	parabola + straight	$w_b = 2aP$ $a = \dfrac{h}{L_1(L_1 + 2L_2)}$	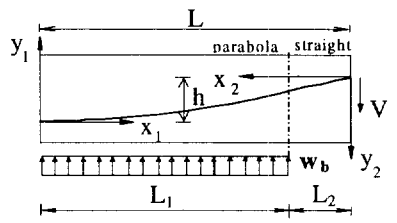
E	parabola + parabola	$w_{b1} = 2aP$ $w_{b2} = 2bP$ $a = \dfrac{h}{L_1 L}$ $b = \dfrac{h}{L_2^2 + L_1 L_2}$	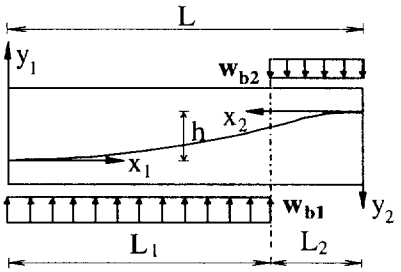
F	parab. + straight +parab.	$w_{b1} = 2aP$ $w_{b2} = 2cP$ $a = \dfrac{h}{2L_1L_2 + L_1^2}$ $c = \dfrac{h}{L_3(2L_2 + L_1 + L_3)}$	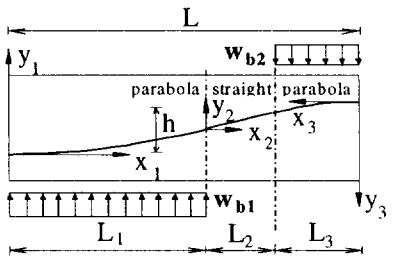

3 ANALYSIS OF NONLINEAR COMPOSITE CROSS-SECTION

The equilibrium of internal and external forces for a nonlinear cross-section is achieved by iteration in which loads are applied in small increments and the solution is obtained by linearization of the problem. Therefore, a linear solution is presented first before presenting the nonlinear solution algorithm.

3.1 LINEAR CROSS-SECTION

According to elementary bending theory, the axial strain ε in a beam cross-section can be expressed as

$$\varepsilon = \varepsilon_0 + y\kappa \tag{1}$$

where ε_0 denotes the axial strain at the reference plane and κ the curvature of the beam. Vertical coordinate y is positive downwards and its origin is at the reference plane. Using Hooke's law, axial stress σ_i in component i of a composite cross-section comprising m different materials is obtained from

$$\sigma_i = E_i(\varepsilon_0 + y\kappa) \tag{2}$$

where E_i is the elasticity modulus of the material in component i. The resulting normal force N and bending moment M due to the axial stress distribution are obtained from

$$N = \int \sigma dA = \varepsilon_0 \sum_{i=1}^{m} E_i \int_{A_i} dA + \kappa \sum_{i=1}^{m} E_i \int_{A_i} y dA \tag{3}$$

$$M = \int \sigma y dA = \varepsilon_0 \sum_{i=1}^{m} E_i \int_{A_i} y dA + \kappa \sum_{i=1}^{m} E_i \int_{A_i} y^2 dA \tag{4}$$

In Equations 1 - 4 no initial stresses due to temperature, shrinkage, prestressing etc. are taken into account.

3.2 NONLINEAR CROSS-SECTION

A nonlinear elastic material behaviour means that the stress-strain relationship is nonlinear. In such a case, no unique elasticity modulus exists and Equations 2 - 4 cannot be used as such.

In a general case, the equilibrium of forces must be sought by iteration. When iterating, the load is increased in small steps called increments. Assume that at increment k, the strain distribution ε^k is known and the corresponding stress distribution σ^k is in equilibrium with the loading. The object is to determine the strain ε^{k+1} and stress σ^{k+1} at increment $k+1$. This can be done by solving ε_0 and κ from

$$N = \int \sigma dA = \varepsilon_0 \sum_{i=1}^{m} \left(\int E^* dA \right)_i + \kappa \sum_{i=1}^{m} \left(\int E^* y dA \right)_i \tag{5}$$

$$M = \int_A \sigma y dA = \varepsilon_0 \sum_{i=1}^{m} \left(\int E^* y dA \right)_i + \kappa \sum_{i=1}^{m} \left(\int E^* y^2 dA \right)_i \tag{6}$$

where the secant modulus

$$E^* = E^*(\varepsilon) = \frac{\sigma^i(\varepsilon)}{\varepsilon^i} \tag{7}$$

is used instead of the elasticity modulus E. Using this notation, the stress-strain relationship becomes

$$\sigma = E^* \varepsilon = E^* (\varepsilon_0 + y\kappa) \tag{8}$$

Now, knowing ε_0 and κ, ε can be calculated from Equation 1, σ_i from the known stress-strain relationship, and the stress resultants N and M from Equations 5 and 6. Finally, N and M are compared with the normal force and bending moment due to the external loads, respectively. If they are not close enough, E^* is updated to correspond to the latest strain distribution, substituted into Equations 5 and 6, and so on. The iteration is continued until the internal forces calculated from the stress distribution are in equilibrium with the external forces, or until the iteration diverges. This is done for each load increment.

Also the bond-slip between the concrete and the steel sheeting, when present, necessitates the equilibrium iteration.

4 LONG-TERM BEHAVIOUR OF CONCRETE

The strain of the concrete comprises an instantaneous and a time-dependent part. The instantaneous strain, also called elastic strain, develops instantaneously when the structure is loaded. The time-dependent part grows gradually with time. The time-dependent strain is due to the creep and shrinkage of the concrete as well as to the relaxation of the prestressing steel.

To simplify calculations, the total strain of the concrete at time t is presented as

$$\varepsilon_c(t) = \varepsilon_{c,e}(t) + \varepsilon_{c,c}(t) + \varepsilon_{c,sh}(t) + \varepsilon_{c,T}(t) \tag{9}$$

where $\varepsilon_{c,e}$, $\varepsilon_{c,c}$, $\varepsilon_{c,sh}$ and $\varepsilon_{c,T}$ denote the elastic strain, the strain due to the creep, the strain due to the shrinkage and the strain due to the temperature change, respectively. In the following, $\varepsilon_{c,T}$ is ignored and the other strain components are regarded as independent of each other. They are first calculated separately and then superimposed.

The total strain of the concrete can also be expressed as a sum of two components

$$\varepsilon_c(t) = \varepsilon_{c,n}(t) + \varepsilon_{c,\sigma}(t) \tag{10}$$

where $\varepsilon_{c,\sigma}(t)$ depends on the stress and $\varepsilon_{c,n}(t)$ does not. The stress affects the instantaneous strain and the creep strain in time interval $t_0 \ldots t$, i.e.

$$\varepsilon_{c,\sigma}(t) = \varepsilon_{c,e}(t) + \varepsilon_{c,c}(t) \tag{11}$$

The total strain at time t due to the initial stress $\sigma_c(t_0)$ at time t_0 and the varying stress in the interval $t_0 \ldots t$ is obtained from

$$\varepsilon_{c,\sigma}(t) = J(t,t_0)\sigma_c(t_0) + \int_{t_0}^{t} J(t,t')\frac{\partial \sigma_c(t')}{\partial t'}dt', \tag{12}$$

where $J(t,t_0)$ is the creep function. In the program,

$$J(t,t_0) = \frac{1}{E_c(t_0)} + \frac{\varphi(t,t_0)}{E_{c28}} \tag{13}$$

taken from CEB-FIP Model Code 90 [3] is used. See also the CEB report [2].

In 1967, Trost [10] introduced a practical method for predicting creep strains. The method was later developed by Bazant [1] who called it "Age-Adjusted Effective Modulus Method". According to this method, the integral in Equation 12 can in many cases be replaced by a simpler algebraic approximation. This can be seen from

$$\int_{t_0}^{t} J(t,t')\frac{\partial \sigma_c(t')}{\partial t'}dt' = \int_{t_0}^{t}\left[\frac{1}{E_c(t_0)} + \left(\frac{\varphi(t,t')}{E_{c28}}\right)\right]\frac{\partial \sigma_c(t')}{\partial t'}dt'$$
$$= \int_{t_0}^{t}\left[\frac{1}{E_c(t_0)} + \chi(t,t_0)\left(\frac{\varphi(t,t_0)}{E_{c28}}\right)\right]\frac{\partial \sigma_c(t')}{\partial t'}dt' \qquad (14)$$
$$= \frac{\Delta\sigma_c(t)}{E_c(t_0)}\left[1 + \chi(t,t_0)\left(\frac{E_c(t_0)}{E_{c28}}\right)\varphi(t,t_0)\right]$$

where φ is the creep coefficient and the aging coefficient $\chi(t,t_0)$ has to be chosen properly. It is constant in time interval $t_0 \ldots t$ and depends on the loading history. If $\Delta\sigma_c(t)$ is not equal to zero, $\chi(t,t_0)$ can in principle always be determined. By introducing the terms effective elasticity modulus, or simply effective modulus,

$$E_{c,e}(t,t_0) = \frac{1}{J(t,t_0)} = \frac{E_c(t_0)}{1 + \left(\frac{E_c(t_0)}{E_{c28}}\right)\varphi(t,t_0)} \qquad (15)$$

and age-adjusted effective elasticity modulus,

$$\bar{E}_{c,e}(t,t_0) = \frac{E_c(t_0)}{1 + \chi(t,t_0)\left(\frac{E_c(t_0)}{E_{c28}}\right)\varphi(t,t_0)} \qquad (16)$$

equation

$$\varepsilon_c(t) = \frac{\sigma_c(t_0)}{E_c(t_0)}\left[1 + \left(\frac{E_c(t_0)}{E_{c28}}\right)\varphi(t,t_0)\right]$$
$$+ \frac{\Delta\sigma_c(t)}{E_c(t_0)}\left[1 + \chi(t,t_0)\left(\frac{E_c(t_0)}{E_{c28}}\right)\varphi(t,t_0)\right] \qquad (17)$$

can be written in the form

$$\varepsilon_c(t) = \frac{\sigma_c(t_0)}{E_{c,e}(t,t_0)} + \frac{\Delta\sigma_c(t)}{\bar{E}_{c,e}(t,t_0)} \qquad (18)$$

In Equation 18 the strain at time t consists of two components. The first one is the instantaneous strain at time t_0 due to the stress $\sigma_c(t_0)$. The other represents the strain change due to the stress increment $\Delta\sigma_c(t)$ in time interval $t_0 \ldots t$.

5 LONG-TERM STRAINS AND STRESSES IN A COMPOSITE SLAB

It is assumed that the falsework and moulds are removed after tensioning the strands, and that the concrete remains uncracked during the tensioning process and under working loads.

5.1 LONG-TERM STRAINS

Consider the long-term deformation of the composite slab cross-section. In addition to the instantaneous strain $\varepsilon_i(t_0) = \varepsilon_0(t_0) + \kappa(t_0) y_i$ due to the external loads, strain due to the creep and shrinkage of the concrete, and to the relaxation of the prestressing steel, arises in a prestressed composite slab. The non-homogeneity of composite cross-sections makes the direct application of creep and shrinkage models complicated. The steel neither creeps nor shrinks but rather reduces the creep and shrinkage of the concrete.

As first approximation, the strain components are solved from

$$N = \int \sigma dA = \varepsilon_0(t) \sum_{i=1}^{m} \left(\int E_e^* dA \right)_i + \kappa(t) \sum_{i=1}^{m} \left(\int E_e^* y dA \right)_i \tag{19}$$

$$M = \int_A \sigma y dA = \varepsilon_0(t) \sum_{i=1}^{m} \left(\int E_e^* y dA \right)_i + \kappa(t) \sum_{i=1}^{m} \left(\int E_e^* y^2 dA \right)_i \tag{20}$$

where E^*_e is the effective modulus and N and M are the normal force and bending moment, respectively, due to the external loads including the prestressing force. To simplify the calculations, it is assumed that the imposed loads are applied immediately after tensioning.

Equations 19 and 20 ignore the shrinkage of the concrete and the relaxation of the steel. They also overestimate the creep since the structural and reinforcing steel

reduce it. To take these effects into account, a correction term $\Delta\varepsilon_0(t)+\Delta\kappa(t)y_i$ is added. The total strain is obtained from

$$\varepsilon_i(t)=\left[\varepsilon_0(t)+\kappa(t)y_i\right]+\left[\Delta\varepsilon_0(t)+\Delta\kappa(t)y_i\right] \tag{21}$$

As an example, consider the shrinkage. Subscript c refers to a force or moment exerted to the concrete cross-section. The strain change due to the shrinkage is calculated using superposition as follows (cf. Fig. 3):

1. Detach the concrete from the steel and allow shrinkage to take place freely in the concrete.
2. Apply to the concrete section an extra normal force ΔN_c and bending moment ΔM_c, hereafter called virtual forces, that make the strain of the concrete equal to the strain before shrinkage started.
3. Attach the concrete to the steel. Note that ΔN_c and ΔM_c are still respectively pulling and bending the concrete cross-section. Replace ΔN_c and ΔM_c with an equivalent system of virtual forces ΔN and ΔM, where ΔN acts along the chosen reference plane of the composite cross-section.
4. Apply $-\Delta N$ and $-\Delta M$ to the composite cross-section.

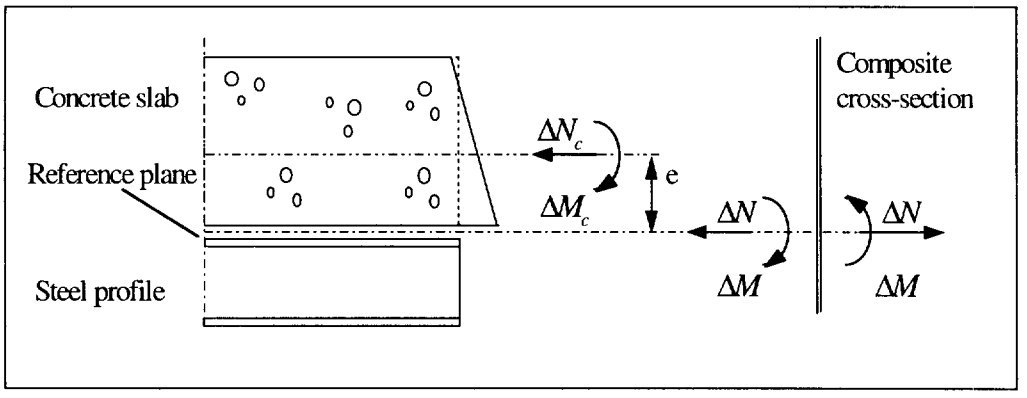

Fig. 3. Virtual forces ΔN_c and ΔM_c preventing free shrinkage and an equivalent system ΔN and ΔM where the normal force acts along the reference plane of the composite section.

The virtual forces are calculated from

$$\begin{Bmatrix}\Delta N\\ \Delta M\end{Bmatrix}_{sh} = \varepsilon_{c,sh}(t,t_0)\begin{Bmatrix}\sum_i\left(\int \bar{E}^*_{c,e}(t,t_0)dA\right)_i\\ \sum_i\left(\int \bar{E}^*_{c,e}(t,t_0)ydA\right)_i\end{Bmatrix} \tag{22}$$

where $\varepsilon_{c,sh}(t,t_0)$ is the free shrinkage in time interval $t_0 \ldots t$ ($\varepsilon_{c,sh}(t,t_0)$ is negative for shrinking and positive for expansion), $\bar{E}^*_{c,e}$ is the effective age-adjusted modulus and the summation is extended over the concrete cross-section. For the creep, the method is similar. The virtual forces restraining the "free" creep are obtained from

$$\begin{Bmatrix}\Delta N\\ \Delta M\end{Bmatrix}_{creep} = \varphi(t,t_0)\begin{bmatrix}\sum_i\left(\int \bar{E}^*_{c,e}(t,t_0)dA\right)_i & \sum_i\left(\int \bar{E}^*_{c,e}(t,t_0)ydA\right)_i\\ \sum_i\left(\int \bar{E}^*_{c,e}(t,t_0)ydA\right)_i & \sum_i\left(\int \bar{E}^*_{c,e}(t,t_0)y^2dA\right)_i\end{bmatrix}\begin{Bmatrix}\varepsilon_0(t_0)\\ \kappa(t_0)\end{Bmatrix} \tag{23}$$

Again, the summation is extended over the concrete cross-section. The strain at time t_0 multiplied by $\varphi(t,t_0)$ represents the "free" creep.

The forces restraining the strains due to the relaxation of the prestressing tendons are calculated from

$$\begin{Bmatrix}\Delta N\\ \Delta M\end{Bmatrix}_{rel} = -\sum_i\begin{Bmatrix}A_{ps}\Delta\bar{\sigma}_{pr}\\ A_{ps}y_{ps}\Delta\bar{\sigma}_{pr}\end{Bmatrix}_i \tag{24}$$

where A_{ps}, y_{ps} and $\Delta\bar{\sigma}_{pr}$ are the cross-sectional area of tendon i, distance of tendon i from the reference plane of the composite cross-section, and change of stress due to relaxation of tendon i. The summation is extended over all tendons. $\Delta\varepsilon_0$ and $\Delta\kappa$ can now be solved from

$$\Delta N = \int \sigma dA = \Delta\varepsilon_0\sum_{i=1}^{m}\left(\int \bar{E}^*_e dA\right)_i + \Delta\kappa\sum_{i=1}^{m}\left(\int \bar{E}^*_e ydA\right)_i \tag{25}$$

$$\Delta M = \int \sigma y dA = \Delta\varepsilon_0 \sum_{i=1}^{m} \left(\int \overline{E}_e^* y dA \right)_i + \Delta\kappa \sum_{i=1}^{m} \left(\int \overline{E}_e^* y^2 dA \right)_i \quad (26)$$

where

$$\begin{Bmatrix} \Delta N \\ \Delta M \end{Bmatrix} = \begin{Bmatrix} \Delta N \\ \Delta M \end{Bmatrix}_{creep} + \begin{Bmatrix} \Delta N \\ \Delta M \end{Bmatrix}_{sh} + \begin{Bmatrix} \Delta N \\ \Delta M \end{Bmatrix}_{rel} \quad (27)$$

Later on ΔN and ΔM, as well as their components due to creep, shrinkage and relaxation, are called *inner forces.*

5.2 LONG-TERM STRESSES

When calculating the long-term stresses of the concrete, the strain obtained from Equations 19 and 20 is multiplied by the effective modulus E^*_e . The stresses due to the virtual forces are calculated by multiplying the strain change $\Delta\varepsilon_0(t) + \Delta\kappa(t) y_i$ by age-adjusted effective modulus $\overline{E}^*_{c,e}(t, t_0)$.

The present program version does not take into account the reduction of the prestressing force due to the creep and shrinkage of the concrete. This has to be modelled by reducing the initial stress.

6 NEW VERSION OF COMPCAL

6.1 GENERAL

The information given in the reports of Daniels [4] and Daniels & alii [5] are not repeated here. In the new program version the same file names are used as in the old one.

6.2 NODAL FORCES DUE TO INNER FORCES

Fig. 4 illustrates the nodal forces ΔN_j and ΔM_j in the FEM model due to the inner forces ΔN and ΔM.

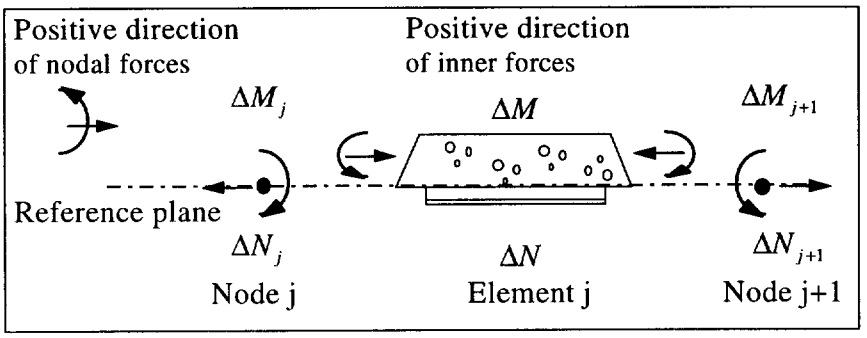

Fig. 4. Nodal forces due to inner forces ΔN and ΔM.

Taking into account the sense of vectors results in the following nodal forces

$$\begin{aligned}
\Delta N_j &= -\left[\Delta N_{creep} + \Delta N_{sh} + \Delta N_{rel}\right] \\
\Delta M_j &= -\left[\Delta M_{creep} + \Delta M_{sh} + \Delta M_{rel}\right] \\
\Delta N_{j+1} &= +\left[\Delta N_{creep} + \Delta N_{sh} + \Delta N_{rel}\right] \\
\Delta M_{j+1} &= +\left[\Delta M_{creep} + \Delta M_{sh} + \Delta M_{rel}\right]
\end{aligned} \tag{28}$$

6.3 ADDED AND CHANGED MODULES IN COMPCAL

Fig. 5 shows the relation of the new program modules to the old ones. A new main program COMPT has been written and the old main program MAIN is now a subroutine.

Subroutine BALANCE calculates the vertical and horizontal loads due to the tendon geometry and tendon forces using load-balancing method.

Subroutine TIMEC calculates the parameters which are independent of time. Time-dependent variables are calculated in subroutine TIMEV.

Subroutine DFORCE determines the intermal forces, nodal forces and moments due to creep, shrinkage and relaxation.

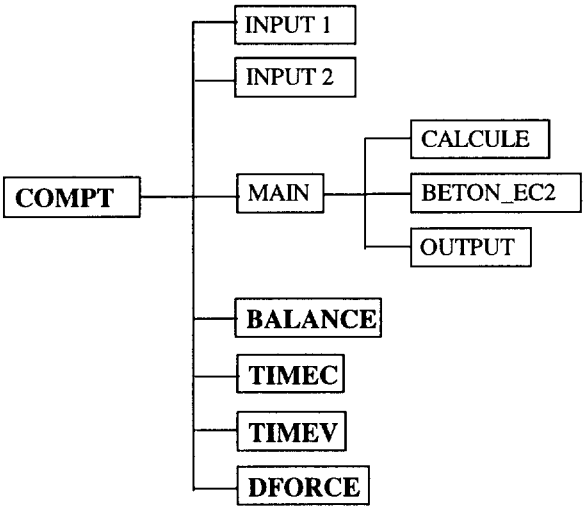

Fig. 5. Added and changed modules. Names of new modules are in bold type.

7 EXAMPLE: TWO-SPAN SLAB PRESTRESSED WITH PARABOLIC TENDONS

The continuous two-span slab shown in Figs 6 and 7 is reinforced using 12 mm bars and prestressed with unbonded parabolic tendons. The concrete is cast on a 0.9 mm thick profiled steel sheeting.

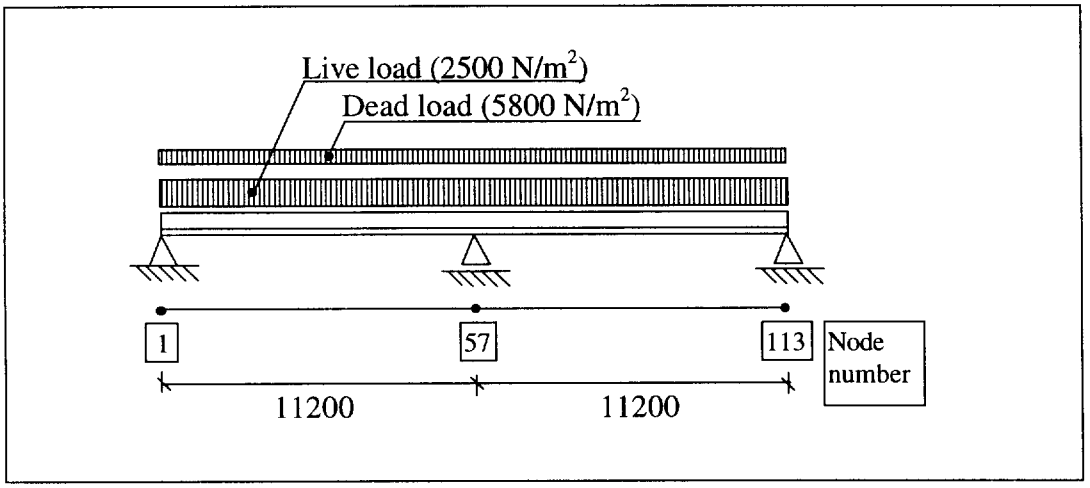

Fig. 6. Structural model.

Nodal coordinates, loads, position, restraints and slip allowance are defined in file NOM5, cf. Appendix A. The structure is subjected to uniform dead and live load. Three supports are assumed, located at the 1st, 57th and 113th nodes. Neither slip restraints nor concentrated connectors are used. Two different cross-section types, A and B, are used. In A, reinforcement is located at the bottom, and in B is used at the intermediate support, at the top of the slab.

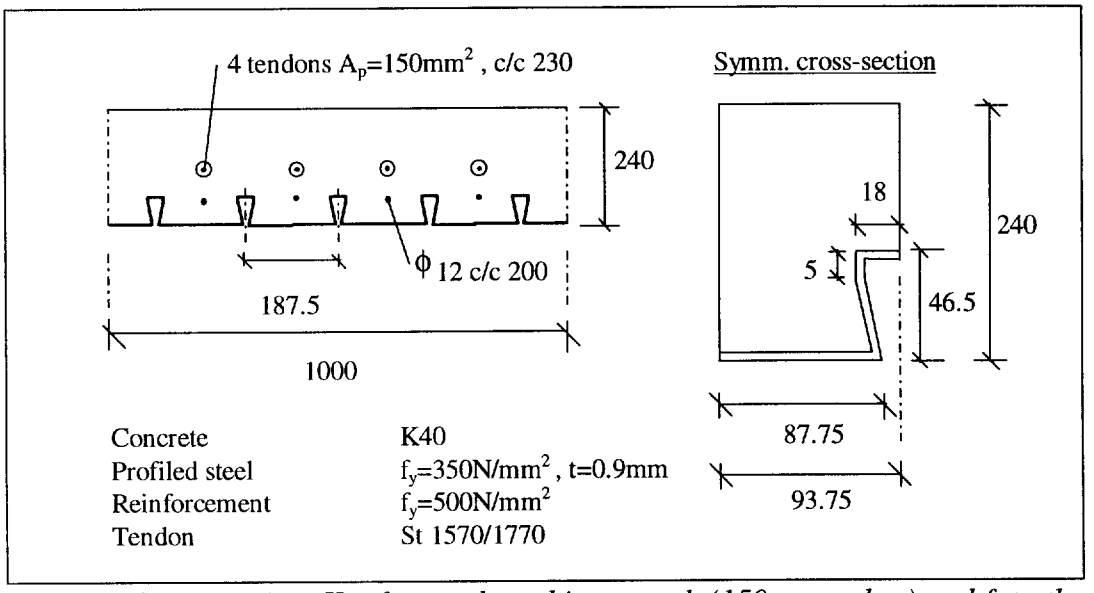

Fig. 7. Cross-section. K refers to the cubic strength (150 mm cubes) and f_y to the yield strength.

Values defining cross-sectional and material properties are given in input files NOM1, NOM2, NOM3 ja NOM4. The input file for cross-section type A is shown in Appendix B. The profile is modelled with seven cut heights. Values for concreted and free edge of the profile are listed in Table 2. In mid-span and at the intermediate support, reinforcements ϕ 12 c/c 200 and ϕ 12 c/c 100 are located at a distance of 44 mm and 204 mm from the bottom fibre of the slab, respectively.

Table 2. Coordinates defining the free and concreted edges of the profile (cf. Fig. 7).

Free edge			Concreted edge		
Node	x [mm]	y [mm]	Node	x [mm]	y [mm]
1	0	0	1	0	0
2	87.8	0	2	0	0.9
3	80.8	41.5	3	86.9	0.9
4	75.8	41.5	4	79.9	40.6
5	75.8	46.5	5	74.9	40.6
6	93.8	46.5	6	74.9	47.4
7	93.8	47.4	7	93.8	47.4

Material properties of the concrete, reinforcing steel and profiled steel are given in Fig. 8. The uniform connection between profile and slab is obtained using small scale tests. In the program, slip-shear stress behaviour is modelled by ten points as described Daniels & alii [5]. Initial deformations are calculated using the test model. Due to some convergence problems, long-term deformations are calculated assuming that the uniform connection is very stiff. This should not affect the calculated deflections, because the slip in a slab subjected to service loads is very small.

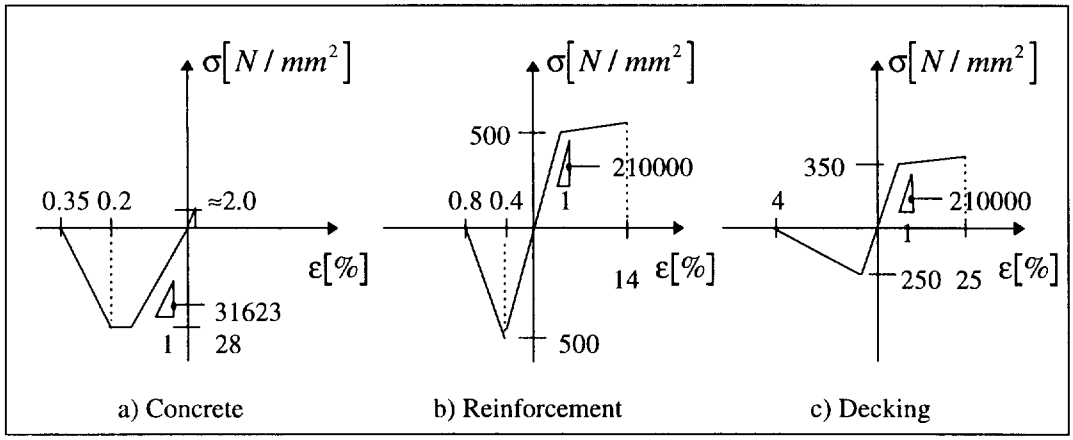

Fig. 8. Stress-strain relationship of materials.

The tendon geometry is depicted in Fig. 9. The initial stress after tensioning is σ_{p0} = 1266.7 N/mm^2. The program ignores the friction between the tendon and the duct.

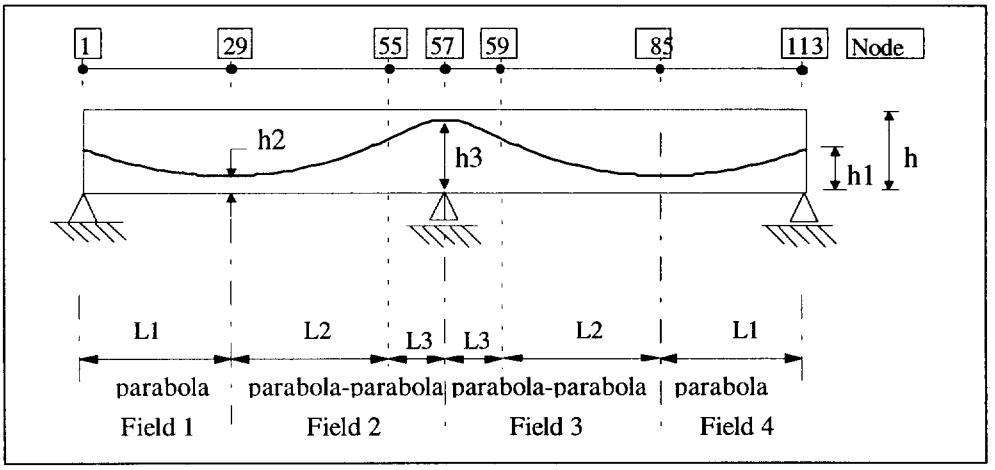

	L1	L2	L3	h	h1	h2	h3
Length[mm]	5600	5300	300	240	115	40	200

Fig. 9. Tendon geometry.

The tendon information is written in input file FILE9 illustrated in Appendix C. The tendon geometry is divided into four fields and for each field the end nodes, geometry type and possible intermediate nodes are given. Location of the tendon is given at the end nodes. The program calculates the coordinates at other points. In Table 3 the tendon geometry is given as written in FILE9.

Table 3. Input data for tendon geometry.

Field	End node		Tendon geometry	Mid-point		Location at end nodes	
	Left end	Right end		1st	2nd	Left end	Right end
1	1	29	B	29	0	115	40
2	29	57	E	55	0	40	200
3	57	85	E	59	0	200	40
4	85	113	B	113	0	40	115

Input file NOM7 contains all internal constant values used in the program. They are described by Daniels & alii [5]. An example is shown in Appendix D.

The calculated results are saved in output file NOM6, see Appendix E. Execution of the program will be terminated if large displacements are indicated, axial stiffness of the slab or profile becomes equal to zero, or the number of iterations

exceeds the maximum value given in file NOM7. The following list documents a COMPT session for the example.

```
COMPT

      INPUT [2.10]    FILE CONTAINING BEAM PROPERTIES
BEA2-12H.DAT
      INPUT [2.10]    FILE CONTAINING TENDON PROPERTIES
TEN2-12P.DAT
      INPUT [2.20]    FILE CONTAINING CONSTANTS
CONST2.DAT
      INPUT [3.10]    FILE CONTAINING BEAM RESULTS
RES.DAT
      INPUT [4.00]    TITLE (title of program run)
5.5.1996, EXAMPLE OF L=2*11200
      INPUT [5.00]    L.L. FORCE FACTORS, C1,C2
1.,0.
      INPUT [6.00]    L.L. MOMENT FACTORS, C3,C4
0.,0.
      VALUES OK (0=OK, INPUT FALSE INPUT # 1...6)
0
      INPUT           RELATIVE HUMIDITY
70.
      INPUT           # OF  TIME STEPS
5
      INPUT           POINTS OF TIME IN DAYS, T1=PRESTRESSING
      T1=
3.
      T2=
30.
      T3=
180.
      T4=
360.
      T5=
1800.
      INPUT           FILE CONTAINING 1st PROFILE PROPERTIES
HOL2409J.DAT
      INPUT           # OF DIVISIONS FOR 1st PROFILE
                      (cr=10   NOTE: NSP must be between 2 and 99)
10
      INPUT           FILE CONTAINING 2nd PROFILE PROPERTIES
HOL24T9J.DAT
      INPUT           # OF DIVISIONS FOR 2nd PROFILE
                      (cr=10   NOTE: NSP must be between 2 and 99)
10
      INPUT           FILE CONTAINING 1st SLAB PROPERTIES
```

```
HOL2409J.DAT
      INPUT          # OF DIVISIONS FOR 1st SLAB
                     (cr=10   NOTE: NSP must be between 2 and 99)
10
      INPUT          FILE CONTAINING 2nd SLAB PROPERTIES
HOL24T9J.DAT
      INPUT          # OF DIVISIONS FOR 2nd SLAB
                     (cr=10   NOTE: NSP must be between 2 and 99)
10
```

The calculated deflections are shown in Figs 10-12. In Fig. 10 two curves with two different values of prestress are depicted. Such parametric studies are necessary since the present program neither takes into account the increase in the tendon stress due to the deflection nor the decrease due to the creep and shrinkage of the concrete. For example, when simulating a loading test, the curve with initial prestress is followed until the concrete cracks in flexure. Thereafter, the curve with a higher prestress (corresponds to increased stress in the tendon) is closer to the real behaviour.

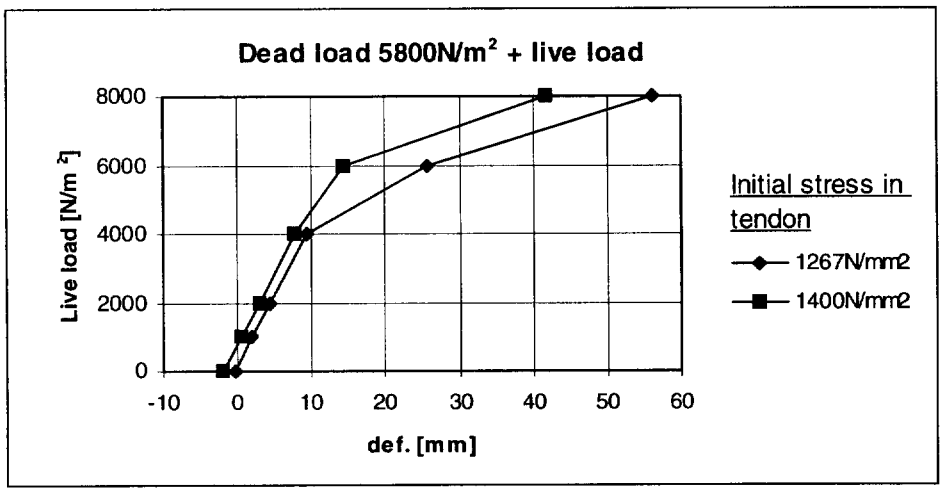

Fig. 10. Initial deflection of slab.

The load-deflection curves shown in Figs 11 and 12 are calculated using initial prestress equal to 1267 N/mm^2.

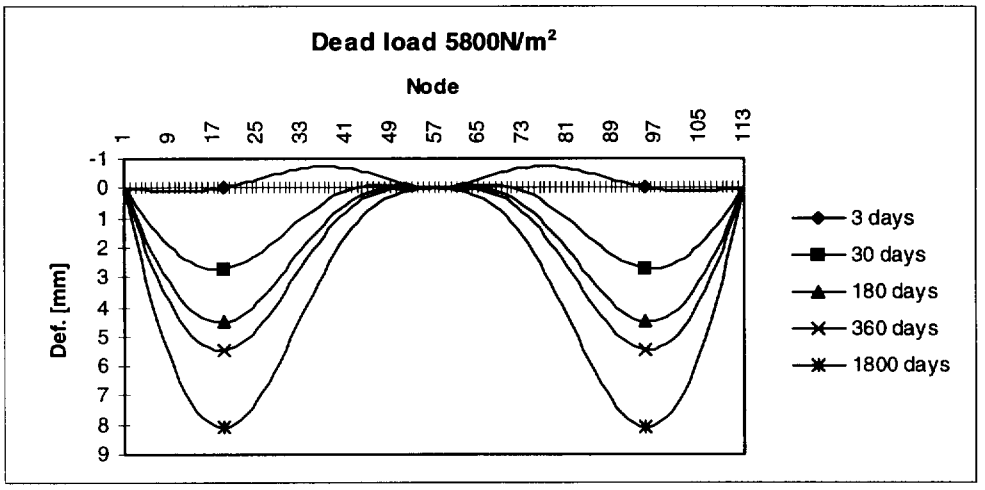

Fig. 11. Deflection of slab due to dead load 5800 N/m².

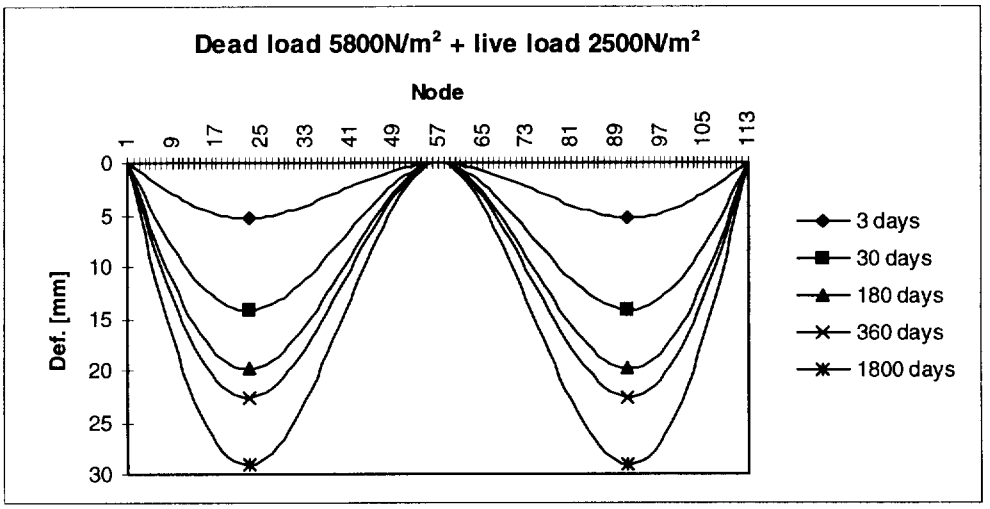

Fig. 12. Deflection of slab due to dead load 5800 N/m² and live load 2500 N/m².

8 DISCUSSION

A method for analysing the long-term behaviour of post-tensioned composite slabs has been proposed and programmed. The well-known load-balancing method has been applied when modelling the effects of post-tensioning.

An example of use of the program is presented. Due to missing experimental data, the analytical long-term deflections could not be compared with the test results. In this sense, verification of the program has been purely formal.

In addition to clarification of the present version of the computer code, the following improvements should be considered when developing the program further:

1. Effect of creep and shrinkage on loads due to tendon forces
2. Effect of deflection on the stress of tendons when the concrete is cracked
3. Free choice of the tensile strength of concrete. At present the tensile strength cannot be given as data.
4. Thorough testing of the program.

LITERATURE

1. Bazant, Z.P. Prediction of concrete creep effects using age-adjusted effective modulus method. ACI Journal, April 1972.

2. CEB. Evaluation of the time dependent behaviour of concrete. Paris: Comité Européen du Béton, September 1990. Bulletin d'Information No. 199.

3. CEB. CEB-FIP Model Code 1990. Vienna: Comité Européen du Béton, July 1991. Bulletin d'Information No. 203, 204, 205.

4. Daniels, B.J. Comportement et capacité portante des dalles mixtes: Modélisation mathématique et et etude expérimentale. Lausanne: Ecole polytechnique fédérale de Lausanne 1990. Thèse No 895. 100 p.

5. Daniels, B.J., Nussbaumer, A. and Crisinel, M. Non-linear analysis of composite members in bending and shear. Lausanne: Ecole polytechnique fédérale de Lausanne, 1989. Publication ICOM 223. 96 p.

6. ENV 1992-1-1. Eurocode 2, Design of concrete structures. In Finnish: Helsinki 1994.

7. Lin, T. Y. & Burns, N. H. Design of prestressed concrete structures. New York: John Wiley & Sons, 1982. 646 p. ISBN 0-471-86724-1

8. Malaska, M. Long-term behaviour of steel-concrete composite slabs prestressed with unbonded tendons (in Finnish). Espoo: Helsinki University of Technology, Faculty of Civil Engineering and Surveying, 1996. Master's Thesis. 64 p. + app. 8 p.

9. Tossavainen, M. Creating tendon geometry for a post-tensioned bridge beam and the forces due to the tensioning (in Finnish). Espoo: Helsinki University of Technology, Institute of Bridge Construction, 1991. Master's Thesis.

10. Trost, H. Auswirkungen des Superpositionsprinzips auf Kriech- und Relaxations-probleme bei Beton- und Spannbeton. Beton- und Stahlbetonbau 62, 1967. H. 10, p. 230 - 238 and H. 11, pp. 261 -269.

FILE NOM5: NODAL INFORMATION, SLIP ALLOWANCE AND SHEAR CONNECTION.

1) TITLE OF DATA FILE

```
EXAMPLE FOR COMPOSITE SLAB (L=2*11200), DL=5800N/m2
```

2) NUMBER OF NODES

```
113
```

3) Y-COORDINATES OF NODES , DX=200mm

```
0.000000000E+00 0.200000000E+03 0.400000000E+03 0.600000000E+03 0.800000000E+03
0.100000000E+04 0.120000000E+04 0.140000000E+04 0.160000000E+04 0.180000000E+04
0.200000000E+04 0.220000000E+04 0.240000000E+04 0.260000000E+04 0.280000000E+04
0.300000000E+04 0.320000000E+04 0.340000000E+04 0.360000000E+04 0.380000000E+04
0.400000000E+04 0.420000000E+04 0.440000000E+04 0.460000000E+04 0.480000000E+04
0.500000000E+04 0.520000000E+04 0.540000000E+04 0.560000000E+04 0.580000000E+04
0.600000000E+04 0.620000000E+04 0.640000000E+04 0.660000000E+04 0.680000000E+04
0.700000000E+04 0.720000000E+04 0.740000000E+04 0.760000000E+04 0.780000000E+04
0.800000000E+04 0.820000000E+04 0.840000000E+04 0.860000000E+04 0.880000000E+04
0.900000000E+04 0.920000000E+04 0.940000000E+04 0.960000000E+04 0.980000000E+04
0.100000000E+05 0.102000000E+05 0.104000000E+05 0.106000000E+05 0.109000000E+05
0.110000000E+05 0.112000000E+05 0.114000000E+05 0.115000000E+05 0.118000000E+05
0.120000000E+05 0.122000000E+05 0.124000000E+05 0.126000000E+05 0.128000000E+05
0.130000000E+05 0.132000000E+05 0.134000000E+05 0.136000000E+05 0.138000000E+05
0.140000000E+05 0.142000000E+05 0.144000000E+05 0.146000000E+05 0.148000000E+05
0.150000000E+05 0.152000000E+05 0.154000000E+05 0.156000000E+05 0.158000000E+05
0.160000000E+05 0.162000000E+05 0.164000000E+05 0.166000000E+05 0.168000000E+05
0.170000000E+05 0.172000000E+05 0.174000000E+05 0.176000000E+05 0.178000000E+05
0.180000000E+05 0.182000000E+05 0.184000000E+05 0.186000000E+05 0.188000000E+05
0.190000000E+05 0.192000000E+05 0.194000000E+05 0.196000000E+05 0.198000000E+05
0.200000000E+05 0.202000000E+05 0.204000000E+05 0.206000000E+05 0.208000000E+05
0.210000000E+05 0.212000000E+05 0.214000000E+05 0.216000000E+05 0.218000000E+05
0.220000000E+05 0.222000000E+05 0.224000000E+05
```

4) VERTICAL SUPPORTS (0.=NO, 1.=YES)

```
0.100000000E+01 0.000000000E+00 0.000000000E+00 0.000000000E+00 0.000000000E+00
0.000000000E+00 0.000000000E+00 0.000000000E+00 0.000000000E+00 0.000000000E+00
0.000000000E+00 0.000000000E+00 0.000000000E+00 0.000000000E+00 0.000000000E+00
0.000000000E+00 0.000000000E+00 0.000000000E+00 0.000000000E+00 0.000000000E+00
0.000000000E+00 0.000000000E+00 0.000000000E+00 0.000000000E+00 0.000000000E+00
0.000000000E+00 0.000000000E+00 0.000000000E+00 0.000000000E+00 0.000000000E+00
0.000000000E+00 0.000000000E+00 0.000000000E+00 0.000000000E+00 0.000000000E+00
0.000000000E+00 0.000000000E+00 0.000000000E+00 0.000000000E+00 0.000000000E+00
0.000000000E+00 0.000000000E+00 0.000000000E+00 0.000000000E+00 0.000000000E+00
0.000000000E+00 0.000000000E+00 0.000000000E+00 0.000000000E+00 0.000000000E+00
0.000000000E+00 0.000000000E+00 0.000000000E+00 0.000000000E+00 0.000000000E+00
0.000000000E+00 0.100000000E+01 0.000000000E+00 0.000000000E+00 0.000000000E+00
0.000000000E+00 0.000000000E+00 0.000000000E+00 0.000000000E+00 0.000000000E+00
0.000000000E+00 0.000000000E+00 0.000000000E+00 0.000000000E+00 0.000000000E+00
0.000000000E+00 0.000000000E+00 0.000000000E+00 0.000000000E+00 0.000000000E+00
0.000000000E+00 0.000000000E+00 0.000000000E+00 0.000000000E+00 0.000000000E+00
0.000000000E+00 0.000000000E+00 0.000000000E+00 0.000000000E+00 0.000000000E+00
0.000000000E+00 0.000000000E+00 0.000000000E+00 0.000000000E+00 0.000000000E+00
0.000000000E+00 0.000000000E+00 0.000000000E+00 0.000000000E+00 0.000000000E+00
0.000000000E+00 0.000000000E+00 0.000000000E+00 0.000000000E+00 0.000000000E+00
0.000000000E+00 0.000000000E+00 0.000000000E+00 0.000000000E+00 0.000000000E+00
0.000000000E+00 0.000000000E+00 0.000000000E+00 0.000000000E+00 0.000000000E+00
0.000000000E+00 0.000000000E+00 0.100000000E+01
```

5) ROTATIONAL SUPPORT (0.=NO, 1.=YES)

```
0.000000000E+00 0.000000000E+00 0.000000000E+00 0.000000000E+00 0.000000000E+00
```

0.000000000E+00 0.000000000E+00 0.000000000E+00 0.000000000E+00 0.000000000E+00
0.000000000E+00 0.000000000E+00 0.000000000E+00 0.000000000E+00 0.000000000E+00
0.000000000E+00 0.000000000E+00 0.000000000E+00 0.000000000E+00 0.000000000E+00
0.000000000E+00 0.000000000E+00 0.000000000E+00 0.000000000E+00 0.000000000E+00
0.000000000E+00 0.000000000E+00 0.000000000E+00 0.000000000E+00 0.000000000E+00
0.000000000E+00 0.000000000E+00 0.000000000E+00 0.000000000E+00 0.000000000E+00
0.000000000E+00 0.000000000E+00 0.000000000E+00 0.000000000E+00 0.000000000E+00
0.000000000E+00 0.000000000E+00 0.000000000E+00 0.000000000E+00 0.000000000E+00
0.000000000E+00 0.000000000E+00 0.000000000E+00 0.000000000E+00 0.000000000E+00
0.000000000E+00 0.000000000E+00 0.000000000E+00 0.000000000E+00 0.000000000E+00
0.000000000E+00 0.000000000E+00 0.000000000E+00 0.000000000E+00 0.000000000E+00
0.000000000E+00 0.000000000E+00 0.000000000E+00 0.000000000E+00 0.000000000E+00
0.000000000E+00 0.000000000E+00 0.000000000E+00 0.000000000E+00 0.000000000E+00
0.000000000E+00 0.000000000E+00 0.000000000E+00 0.000000000E+00 0.000000000E+00
0.000000000E+00 0.000000000E+00 0.000000000E+00 0.000000000E+00 0.000000000E+00
0.000000000E+00 0.000000000E+00 0.000000000E+00 0.000000000E+00 0.000000000E+00
0.000000000E+00 0.000000000E+00 0.000000000E+00 0.000000000E+00 0.000000000E+00
0.000000000E+00 0.000000000E+00 0.000000000E+00 0.000000000E+00 0.000000000E+00
0.000000000E+00 0.000000000E+00 0.000000000E+00 0.000000000E+00 0.000000000E+00
0.000000000E+00 0.000000000E+00 0.000000000E+00 0.000000000E+00 0.000000000E+00
0.000000000E+00 0.000000000E+00 0.000000000E+00 0.000000000E+00 0.000000000E+00
0.000000000E+00 0.000000000E+00 0.000000000E+00

6) SLIP AT INTERFACE (0.=SLIP ALLOWED, 1.=NO SLIP)
0.000000000E+00 0.000000000E+00 0.000000000E+00 0.000000000E+00 0.000000000E+00
0.000000000E+00 0.000000000E+00 0.000000000E+00 0.000000000E+00 0.000000000E+00
0.000000000E+00 0.000000000E+00 0.000000000E+00 0.000000000E+00 0.000000000E+00
0.000000000E+00 0.000000000E+00 0.000000000E+00 0.000000000E+00 0.000000000E+00
0.000000000E+00 0.000000000E+00 0.000000000E+00 0.000000000E+00 0.000000000E+00
0.000000000E+00 0.000000000E+00 0.000000000E+00 0.000000000E+00 0.000000000E+00
0.000000000E+00 0.000000000E+00 0.000000000E+00 0.000000000E+00 0.000000000E+00
0.000000000E+00 0.000000000E+00 0.000000000E+00 0.000000000E+00 0.000000000E+00
0.000000000E+00 0.000000000E+00 0.000000000E+00 0.000000000E+00 0.000000000E+00
0.000000000E+00 0.000000000E+00 0.000000000E+00 0.000000000E+00 0.000000000E+00
0.000000000E+00 0.000000000E+00 0.000000000E+00 0.000000000E+00 0.000000000E+00
0.000000000E+00 0.000000000E+00 0.000000000E+00 0.000000000E+00 0.000000000E+00
0.000000000E+00 0.000000000E+00 0.000000000E+00 0.000000000E+00 0.000000000E+00
0.000000000E+00 0.000000000E+00 0.000000000E+00 0.000000000E+00 0.000000000E+00
0.000000000E+00 0.000000000E+00 0.000000000E+00 0.000000000E+00 0.000000000E+00
0.000000000E+00 0.000000000E+00 0.000000000E+00 0.000000000E+00 0.000000000E+00
0.000000000E+00 0.000000000E+00 0.000000000E+00 0.000000000E+00 0.000000000E+00
0.000000000E+00 0.000000000E+00 0.000000000E+00 0.000000000E+00 0.000000000E+00
0.000000000E+00 0.000000000E+00 0.000000000E+00 0.000000000E+00 0.000000000E+00
0.000000000E+00 0.000000000E+00 0.000000000E+00 0.000000000E+00 0.000000000E+00
0.000000000E+00 0.000000000E+00 0.000000000E+00 0.000000000E+00 0.000000000E+00
0.000000000E+00 0.000000000E+00 0.000000000E+00 0.000000000E+00 0.000000000E+00
0.000000000E+00 0.000000000E+00 0.000000000E+00

7) NODAL DEAD LOADS (5800N/m2)
0.580000000E+03 0.116000000E+04 0.116000000E+04 0.116000000E+04 0.116000000E+04
0.116000000E+04 0.116000000E+04 0.116000000E+04 0.116000000E+04 0.116000000E+04
0.116000000E+04 0.116000000E+04 0.116000000E+04 0.116000000E+04 0.116000000E+04
0.116000000E+04 0.116000000E+04 0.116000000E+04 0.116000000E+04 0.116000000E+04
0.116000000E+04 0.116000000E+04 0.116000000E+04 0.116000000E+04 0.116000000E+04
0.116000000E+04 0.116000000E+04 0.116000000E+04 0.116000000E+04 0.116000000E+04
0.116000000E+04 0.116000000E+04 0.116000000E+04 0.116000000E+04 0.116000000E+04
0.116000000E+04 0.116000000E+04 0.116000000E+04 0.116000000E+04 0.116000000E+04
0.116000000E+04 0.116000000E+04 0.116000000E+04 0.116000000E+04 0.116000000E+04
0.116000000E+04 0.116000000E+04 0.116000000E+04 0.116000000E+04 0.116000000E+04
0.116000000E+04 0.116000000E+04 0.116000000E+04 0.116000000E+04 0.116000000E+04
0.116000000E+04 0.116000000E+04 0.116000000E+04 0.116000000E+04 0.116000000E+04
0.116000000E+04 0.116000000E+04 0.116000000E+04 0.116000000E+04 0.116000000E+04

0.116000000E+04 0.116000000E+04 0.116000000E+04 0.116000000E+04 0.116000000E+04
0.116000000E+04 0.116000000E+04 0.116000000E+04 0.116000000E+04 0.116000000E+04
0.116000000E+04 0.116000000E+04 0.116000000E+04 0.116000000E+04 0.116000000E+04
0.116000000E+04 0.116000000E+04 0.116000000E+04 0.116000000E+04 0.116000000E+04
0.116000000E+04 0.116000000E+04 0.116000000E+04 0.116000000E+04 0.116000000E+04
0.116000000E+04 0.116000000E+04 0.116000000E+04 0.116000000E+04 0.116000000E+04
0.116000000E+04 0.116000000E+04 0.116000000E+04 0.116000000E+04 0.116000000E+04
0.116000000E+04 0.116000000E+04 0.116000000E+04 0.116000000E+04 0.116000000E+04
0.116000000E+04 0.116000000E+04 0.116000000E+04 0.116000000E+04 0.116000000E+04
0.116000000E+04 0.116000000E+04 0.580000000E+03

8) NODAL DEAD LOAD MOMENTS
0.000000000E+00 0.000000000E+00 0.000000000E+00 0.000000000E+00 0.000000000E+00
0.000000000E+00 0.000000000E+00 0.000000000E+00 0.000000000E+00 0.000000000E+00
0.000000000E+00 0.000000000E+00 0.000000000E+00 0.000000000E+00 0.000000000E+00
0.000000000E+00 0.000000000E+00 0.000000000E+00 0.000000000E+00 0.000000000E+00
0.000000000E+00 0.000000000E+00 0.000000000E+00 0.000000000E+00 0.000000000E+00
0.000000000E+00 0.000000000E+00 0.000000000E+00 0.000000000E+00 0.000000000E+00
0.000000000E+00 0.000000000E+00 0.000000000E+00 0.000000000E+00 0.000000000E+00
0.000000000E+00 0.000000000E+00 0.000000000E+00 0.000000000E+00 0.000000000E+00
0.000000000E+00 0.000000000E+00 0.000000000E+00 0.000000000E+00 0.000000000E+00
0.000000000E+00 0.000000000E+00 0.000000000E+00 0.000000000E+00 0.000000000E+00
0.000000000E+00 0.000000000E+00 0.000000000E+00 0.000000000E+00 0.000000000E+00
0.000000000E+00 0.000000000E+00 0.000000000E+00 0.000000000E+00 0.000000000E+00
0.000000000E+00 0.000000000E+00 0.000000000E+00 0.000000000E+00 0.000000000E+00
0.000000000E+00 0.000000000E+00 0.000000000E+00 0.000000000E+00 0.000000000E+00
0.000000000E+00 0.000000000E+00 0.000000000E+00 0.000000000E+00 0.000000000E+00
0.000000000E+00 0.000000000E+00 0.000000000E+00 0.000000000E+00 0.000000000E+00
0.000000000E+00 0.000000000E+00 0.000000000E+00 0.000000000E+00 0.000000000E+00
0.000000000E+00 0.000000000E+00 0.000000000E+00 0.000000000E+00 0.000000000E+00
0.000000000E+00 0.000000000E+00 0.000000000E+00 0.000000000E+00 0.000000000E+00
0.000000000E+00 0.000000000E+00 0.000000000E+00 0.000000000E+00 0.000000000E+00
0.000000000E+00 0.000000000E+00 0.000000000E+00 0.000000000E+00 0.000000000E+00
0.000000000E+00 0.000000000E+00 0.000000000E+00 0.000000000E+00 0.000000000E+00
0.000000000E+00 0.000000000E+00 0.000000000E+00

9) INITIAL NODAL LIVE LOADS (2500N/m2)
0.250000000E+03 0.500000000E+03 0.500000000E+03 0.500000000E+03 0.500000000E+03
0.500000000E+03 0.500000000E+03 0.500000000E+03 0.500000000E+03 0.500000000E+03
0.500000000E+03 0.500000000E+03 0.500000000E+03 0.500000000E+03 0.500000000E+03
0.500000000E+03 0.500000000E+03 0.500000000E+03 0.500000000E+03 0.500000000E+03
0.500000000E+03 0.500000000E+03 0.500000000E+03 0.500000000E+03 0.500000000E+03
0.500000000E+03 0.500000000E+03 0.500000000E+03 0.500000000E+03 0.500000000E+03
0.500000000E+03 0.500000000E+03 0.500000000E+03 0.500000000E+03 0.500000000E+03
0.500000000E+03 0.500000000E+03 0.500000000E+03 0.500000000E+03 0.500000000E+03
0.500000000E+03 0.500000000E+03 0.500000000E+03 0.500000000E+03 0.500000000E+03
0.500000000E+03 0.500000000E+03 0.500000000E+03 0.500000000E+03 0.500000000E+03
0.500000000E+03 0.500000000E+03 0.500000000E+03 0.500000000E+03 0.500000000E+03
0.500000000E+03 0.500000000E+03 0.500000000E+03 0.500000000E+03 0.500000000E+03
0.500000000E+03 0.500000000E+03 0.500000000E+03 0.500000000E+03 0.500000000E+03
0.500000000E+03 0.500000000E+03 0.500000000E+03 0.500000000E+03 0.500000000E+03
0.500000000E+03 0.500000000E+03 0.500000000E+03 0.500000000E+03 0.500000000E+03
0.500000000E+03 0.500000000E+03 0.500000000E+03 0.500000000E+03 0.500000000E+03
0.500000000E+03 0.500000000E+03 0.500000000E+03 0.500000000E+03 0.500000000E+03
0.500000000E+03 0.500000000E+03 0.500000000E+03 0.500000000E+03 0.500000000E+03
0.500000000E+03 0.500000000E+03 0.500000000E+03 0.500000000E+03 0.500000000E+03
0.500000000E+03 0.500000000E+03 0.500000000E+03 0.500000000E+03 0.500000000E+03
0.500000000E+03 0.500000000E+03 0.500000000E+03 0.500000000E+03 0.500000000E+03
0.500000000E+03 0.500000000E+03 0.500000000E+03 0.500000000E+03 0.500000000E+03
0.500000000E+03 0.500000000E+03 0.250000000E+03

10) INITIAL NODAL DEAD LOAD MOMENTS

0.000000000E+00 0.000000000E+00 0.000000000E+00 0.000000000E+00 0.000000000E+00
0.000000000E+00 0.000000000E+00 0.000000000E+00 0.000000000E+00 0.000000000E+00
0.000000000E+00 0.000000000E+00 0.000000000E+00 0.000000000E+00 0.000000000E+00
0.000000000E+00 0.000000000E+00 0.000000000E+00 0.000000000E+00 0.000000000E+00
0.000000000E+00 0.000000000E+00 0.000000000E+00 0.000000000E+00 0.000000000E+00
0.000000000E+00 0.000000000E+00 0.000000000E+00 0.000000000E+00 0.000000000E+00
0.000000000E+00 0.000000000E+00 0.000000000E+00 0.000000000E+00 0.000000000E+00
0.000000000E+00 0.000000000E+00 0.000000000E+00 0.000000000E+00 0.000000000E+00
0.000000000E+00 0.000000000E+00 0.000000000E+00 0.000000000E+00 0.000000000E+00
0.000000000E+00 0.000000000E+00 0.000000000E+00 0.000000000E+00 0.000000000E+00
0.000000000E+00 0.000000000E+00 0.000000000E+00 0.000000000E+00 0.000000000E+00
0.000000000E+00 0.000000000E+00 0.000000000E+00 0.000000000E+00 0.000000000E+00
0.000000000E+00 0.000000000E+00 0.000000000E+00 0.000000000E+00 0.000000000E+00
0.000000000E+00 0.000000000E+00 0.000000000E+00 0.000000000E+00 0.000000000E+00
0.000000000E+00 0.000000000E+00 0.000000000E+00 0.000000000E+00 0.000000000E+00
0.000000000E+00 0.000000000E+00 0.000000000E+00 0.000000000E+00 0.000000000E+00
0.000000000E+00 0.000000000E+00 0.000000000E+00 0.000000000E+00 0.000000000E+00
0.000000000E+00 0.000000000E+00 0.000000000E+00 0.000000000E+00 0.000000000E+00
0.000000000E+00 0.000000000E+00 0.000000000E+00 0.000000000E+00 0.000000000E+00
0.000000000E+00 0.000000000E+00 0.000000000E+00 0.000000000E+00 0.000000000E+00
0.000000000E+00 0.000000000E+00 0.000000000E+00 0.000000000E+00 0.000000000E+00
0.000000000E+00 0.000000000E+00 0.000000000E+00 0.000000000E+00 0.000000000E+00
0.000000000E+00 0.000000000E+00 0.000000000E+00

11) INITIAL NODAL VERTICAL DISPLACEMENTS
0.000000000E+00 0.000000000E+00 0.000000000E+00 0.000000000E+00 0.000000000E+00
0.000000000E+00 0.000000000E+00 0.000000000E+00 0.000000000E+00 0.000000000E+00
0.000000000E+00 0.000000000E+00 0.000000000E+00 0.000000000E+00 0.000000000E+00
0.000000000E+00 0.000000000E+00 0.000000000E+00 0.000000000E+00 0.000000000E+00
0.000000000E+00 0.000000000E+00 0.000000000E+00 0.000000000E+00 0.000000000E+00
0.000000000E+00 0.000000000E+00 0.000000000E+00 0.000000000E+00 0.000000000E+00
0.000000000E+00 0.000000000E+00 0.000000000E+00 0.000000000E+00 0.000000000E+00
0.000000000E+00 0.000000000E+00 0.000000000E+00 0.000000000E+00 0.000000000E+00
0.000000000E+00 0.000000000E+00 0.000000000E+00 0.000000000E+00 0.000000000E+00
0.000000000E+00 0.000000000E+00 0.000000000E+00 0.000000000E+00 0.000000000E+00
0.000000000E+00 0.000000000E+00 0.000000000E+00 0.000000000E+00 0.000000000E+00
0.000000000E+00 0.000000000E+00 0.000000000E+00 0.000000000E+00 0.000000000E+00
0.000000000E+00 0.000000000E+00 0.000000000E+00 0.000000000E+00 0.000000000E+00
0.000000000E+00 0.000000000E+00 0.000000000E+00 0.000000000E+00 0.000000000E+00
0.000000000E+00 0.000000000E+00 0.000000000E+00 0.000000000E+00 0.000000000E+00
0.000000000E+00 0.000000000E+00 0.000000000E+00 0.000000000E+00 0.000000000E+00
0.000000000E+00 0.000000000E+00 0.000000000E+00 0.000000000E+00 0.000000000E+00
0.000000000E+00 0.000000000E+00 0.000000000E+00 0.000000000E+00 0.000000000E+00
0.000000000E+00 0.000000000E+00 0.000000000E+00 0.000000000E+00 0.000000000E+00
0.000000000E+00 0.000000000E+00 0.000000000E+00 0.000000000E+00 0.000000000E+00
0.000000000E+00 0.000000000E+00 0.000000000E+00 0.000000000E+00 0.000000000E+00
0.000000000E+00 0.000000000E+00 0.000000000E+00 0.000000000E+00 0.000000000E+00
0.000000000E+00 0.000000000E+00 0.000000000E+00

12) INITIAL NODAL ROTATIONS
0.000000000E+00 0.000000000E+00 0.000000000E+00 0.000000000E+00 0.000000000E+00
0.000000000E+00 0.000000000E+00 0.000000000E+00 0.000000000E+00 0.000000000E+00
0.000000000E+00 0.000000000E+00 0.000000000E+00 0.000000000E+00 0.000000000E+00
0.000000000E+00 0.000000000E+00 0.000000000E+00 0.000000000E+00 0.000000000E+00
0.000000000E+00 0.000000000E+00 0.000000000E+00 0.000000000E+00 0.000000000E+00
0.000000000E+00 0.000000000E+00 0.000000000E+00 0.000000000E+00 0.000000000E+00
0.000000000E+00 0.000000000E+00 0.000000000E+00 0.000000000E+00 0.000000000E+00
0.000000000E+00 0.000000000E+00 0.000000000E+00 0.000000000E+00 0.000000000E+00
0.000000000E+00 0.000000000E+00 0.000000000E+00 0.000000000E+00 0.000000000E+00
0.000000000E+00 0.000000000E+00 0.000000000E+00 0.000000000E+00 0.000000000E+00
0.000000000E+00 0.000000000E+00 0.000000000E+00 0.000000000E+00 0.000000000E+00
0.000000000E+00 0.000000000E+00 0.000000000E+00 0.000000000E+00 0.000000000E+00

0.000000000E+00 0.000000000E+00 0.000000000E+00 0.000000000E+00 0.000000000E+00
0.000000000E+00 0.000000000E+00 0.000000000E+00 0.000000000E+00 0.000000000E+00
0.000000000E+00 0.000000000E+00 0.000000000E+00 0.000000000E+00 0.000000000E+00
0.000000000E+00 0.000000000E+00 0.000000000E+00 0.000000000E+00 0.000000000E+00
0.000000000E+00 0.000000000E+00 0.000000000E+00 0.000000000E+00 0.000000000E+00
0.000000000E+00 0.000000000E+00 0.000000000E+00 0.000000000E+00 0.000000000E+00
0.000000000E+00 0.000000000E+00 0.000000000E+00 0.000000000E+00 0.000000000E+00
0.000000000E+00 0.000000000E+00 0.000000000E+00 0.000000000E+00 0.000000000E+00
0.000000000E+00 0.000000000E+00 0.000000000E+00 0.000000000E+00 0.000000000E+00
0.000000000E+00 0.000000000E+00 0.000000000E+00 0.000000000E+00 0.000000000E+00
0.000000000E+00 0.000000000E+00 0.000000000E+00

13) PROFILE CROSS-SECTION TYPE (0.=TYPE "A", 1.=TYPE "B")
0.000000000E+00 0.000000000E+00 0.000000000E+00 0.000000000E+00 0.000000000E+00
0.000000000E+00 0.000000000E+00 0.000000000E+00 0.000000000E+00 0.000000000E+00
0.000000000E+00 0.000000000E+00 0.000000000E+00 0.000000000E+00 0.000000000E+00
0.000000000E+00 0.000000000E+00 0.000000000E+00 0.000000000E+00 0.000000000E+00
0.000000000E+00 0.000000000E+00 0.000000000E+00 0.000000000E+00 0.000000000E+00
0.000000000E+00 0.000000000E+00 0.000000000E+00 0.000000000E+00 0.000000000E+00
0.000000000E+00 0.000000000E+00 0.000000000E+00 0.000000000E+00 0.000000000E+00
0.000000000E+00 0.000000000E+00 0.000000000E+00 0.000000000E+00 0.000000000E+00
0.000000000E+00 0.000000000E+00 0.000000000E+00 0.000000000E+00 0.000000000E+00
0.000000000E+00 0.000000000E+00 0.000000000E+00 0.000000000E+00 0.000000000E+00
0.000000000E+00 0.000000000E+00 0.000000000E+00 0.000000000E+00 0.100000000E+01
0.100000000E+01 0.100000000E+01 0.100000000E+01 0.000000000E+00 0.000000000E+00
0.000000000E+00 0.000000000E+00 0.000000000E+00 0.000000000E+00 0.000000000E+00
0.000000000E+00 0.000000000E+00 0.000000000E+00 0.000000000E+00 0.000000000E+00
0.000000000E+00 0.000000000E+00 0.000000000E+00 0.000000000E+00 0.000000000E+00
0.000000000E+00 0.000000000E+00 0.000000000E+00 0.000000000E+00 0.000000000E+00
0.000000000E+00 0.000000000E+00 0.000000000E+00 0.000000000E+00 0.000000000E+00
0.000000000E+00 0.000000000E+00 0.000000000E+00 0.000000000E+00 0.000000000E+00
0.000000000E+00 0.000000000E+00 0.000000000E+00 0.000000000E+00 0.000000000E+00
0.000000000E+00 0.000000000E+00 0.000000000E+00 0.000000000E+00 0.000000000E+00
0.000000000E+00 0.000000000E+00 0.000000000E+00 0.000000000E+00 0.000000000E+00
0.000000000E+00 0.000000000E+00 0.000000000E+00 0.000000000E+00 0.000000000E+00
0.000000000E+00 0.000000000E+00

14) SLAB CROSS-SECTION TYPE (0.=TYPE "A", 1.=TYPE "B")
0.000000000E+00 0.000000000E+00 0.000000000E+00 0.000000000E+00 0.000000000E+00
0.000000000E+00 0.000000000E+00 0.000000000E+00 0.000000000E+00 0.000000000E+00
0.000000000E+00 0.000000000E+00 0.000000000E+00 0.000000000E+00 0.000000000E+00
0.000000000E+00 0.000000000E+00 0.000000000E+00 0.000000000E+00 0.000000000E+00
0.000000000E+00 0.000000000E+00 0.000000000E+00 0.000000000E+00 0.000000000E+00
0.000000000E+00 0.000000000E+00 0.000000000E+00 0.000000000E+00 0.000000000E+00
0.000000000E+00 0.000000000E+00 0.000000000E+00 0.000000000E+00 0.000000000E+00
0.000000000E+00 0.000000000E+00 0.000000000E+00 0.000000000E+00 0.000000000E+00
0.000000000E+00 0.000000000E+00 0.000000000E+00 0.000000000E+00 0.000000000E+00
0.000000000E+00 0.000000000E+00 0.000000000E+00 0.000000000E+00 0.000000000E+00
0.000000000E+00 0.000000000E+00 0.000000000E+00 0.000000000E+00 0.100000000E+01
0.100000000E+01 0.100000000E+01 0.100000000E+01 0.000000000E+00 0.000000000E+00
0.000000000E+00 0.000000000E+00 0.000000000E+00 0.000000000E+00 0.000000000E+00
0.000000000E+00 0.000000000E+00 0.000000000E+00 0.000000000E+00 0.000000000E+00
0.000000000E+00 0.000000000E+00 0.000000000E+00 0.000000000E+00 0.000000000E+00
0.000000000E+00 0.000000000E+00 0.000000000E+00 0.000000000E+00 0.000000000E+00
0.000000000E+00 0.000000000E+00 0.000000000E+00 0.000000000E+00 0.000000000E+00
0.000000000E+00 0.000000000E+00 0.000000000E+00 0.000000000E+00 0.000000000E+00
0.000000000E+00 0.000000000E+00 0.000000000E+00 0.000000000E+00 0.000000000E+00
0.000000000E+00 0.000000000E+00 0.000000000E+00 0.000000000E+00 0.000000000E+00
0.000000000E+00 0.000000000E+00 0.000000000E+00 0.000000000E+00 0.000000000E+00
0.000000000E+00 0.000000000E+00 0.000000000E+00 0.000000000E+00 0.000000000E+00
0.000000000E+00 0.000000000E+00

15) LOCATION OF ADDITIONAL SHEAR CONNECTION (0.=NO, 1.=YES)

```
0.000000000E+00 0.000000000E+00 0.000000000E+00 0.000000000E+00 0.000000000E+00
0.000000000E+00 0.000000000E+00 0.000000000E+00 0.000000000E+00 0.000000000E+00
0.000000000E+00 0.000000000E+00 0.000000000E+00 0.000000000E+00 0.000000000E+00
0.000000000E+00 0.000000000E+00 0.000000000E+00 0.000000000E+00 0.000000000E+00
0.000000000E+00 0.000000000E+00 0.000000000E+00 0.000000000E+00 0.000000000E+00
0.000000000E+00 0.000000000E+00 0.000000000E+00 0.000000000E+00 0.000000000E+00
0.000000000E+00 0.000000000E+00 0.000000000E+00 0.000000000E+00 0.000000000E+00
0.000000000E+00 0.000000000E+00 0.000000000E+00 0.000000000E+00 0.000000000E+00
0.000000000E+00 0.000000000E+00 0.000000000E+00 0.000000000E+00 0.000000000E+00
0.000000000E+00 0.000000000E+00 0.000000000E+00 0.000000000E+00 0.000000000E+00
0.000000000E+00 0.000000000E+00 0.000000000E+00 0.000000000E+00 0.000000000E+00
0.000000000E+00 0.000000000E+00 0.000000000E+00 0.000000000E+00 0.000000000E+00
0.000000000E+00 0.000000000E+00 0.000000000E+00 0.000000000E+00 0.000000000E+00
0.000000000E+00 0.000000000E+00 0.000000000E+00 0.000000000E+00 0.000000000E+00
0.000000000E+00 0.000000000E+00 0.000000000E+00 0.000000000E+00 0.000000000E+00
0.000000000E+00 0.000000000E+00 0.000000000E+00 0.000000000E+00 0.000000000E+00
0.000000000E+00 0.000000000E+00 0.000000000E+00 0.000000000E+00 0.000000000E+00
0.000000000E+00 0.000000000E+00 0.000000000E+00 0.000000000E+00 0.000000000E+00
0.000000000E+00 0.000000000E+00 0.000000000E+00 0.000000000E+00 0.000000000E+00
0.000000000E+00 0.000000000E+00 0.000000000E+00 0.000000000E+00 0.000000000E+00
0.000000000E+00 0.000000000E+00 0.000000000E+00 0.000000000E+00 0.000000000E+00
0.000000000E+00 0.000000000E+00 0.000000000E+00 0.000000000E+00 0.000000000E+00
0.000000000E+00 0.000000000E+00
```

INPUT FILES NOM1, NOM2, NOM3, NOM4: SECTIONAL AND MATERIAL PROPERTIES.

1) TITLE OF DATA FILE
HOLORIB-2000, t=0.90mm, h=240mm, jäykkä

2) TYPE OF CONCRETE
EC2

3) VALUES DEFINING CONCRETE STRESS-STRAIN BEHAVIOUR(K40)
0.280000000E+02 0.316230000E+05 0.000000000E-02 0.200000000E-02 0.350000000E-02
0.000000000E+00

4) VALUES DEFINING REINFORCEMENT STRESS-STRAIN BEHAVIOUR (500MPa)
0.500000000E+03 0.210000000E+06 0.800000000E-02 0.400000000E-02 0.140000000E+00

5) VALUES DEFINING TENDON STRESS-STRAIN BEHAVIOUR (1570/1770)
0.157000000E+04 0.210000000E+06 0.800000000E-02 0.400000000E-02 0.140000000E+00

6) VALUES DEFINING PROFILE STRESS-STRAIN BEHAVIOUR (350MPa)
0.350000000E+03 0.210000000E+06 0.400000000E-01 0.300000000E-02 0.250000000E+00

7) Wtot,Wsym,Ws, Hpt,Hpl,Htt,Htl
0.100000000E+04 0.937500000E+02 0.159300000E+03 0.473200000E+02 0.000000000E+00
0.240000000E+03 0.820000000E+00

8) # OF CUT HEIGHTS FOR THE PROFILE
7

9) X, Y COORDINATES OF CONCRETED EDGE OF PROFILE
0.000000000E+00 0.000000000E+00 0.869300000E+02 0.799300000E+02 0.749300000E+02
0.749300000E+02 0.937500000E+02

0.000000000E+00 0.820000000E+00 0.820000000E+00 0.406800000E+02 0.406800000E+02
0.473200000E+02 0.473200000E+02

10) X, Y COORDINATES OF UNCONCRETED EDGE OF PROFILE
0.000000000E+00 0.877500000E+02 0.807500000E+02 0.757500000E+02 0.757500000E+02
0.937500000E+02 0.937500000E+02

0.000000000E+00 0.000000000E+00 0.415000000E+02 0.415000000E+02 0.465000000E+02
0.465000000E+02 0.473200000E+02

11) # OF CUT HEIGHTS FOR REINFORCEMENT
2

12) INDIVIDUAL CUT HEIGHTS FOR REINFORCEMENT
0.380000000E+02 0.500000000E+02

13) REINFORCEMENT AREA/Wsym BETWEEN CUT HEIGHTS (12k200)
0.530000000E+02

16) SLIP VALUES FOR PROFILE-SLAB INTERFACE (0.9mm)
0.000000000E+00 0.002000000E+00 0.400000000E+00 0.600000000E+00 0.800000000E+00
0.100000000E+01 0.120000000E+01 0.140000000E+01 0.500000000E+01 0.180000000E+02

17) SHEAR-STRESS VALUES FOR THE PROFILE-SLIP INTERFACE /Wsym)
0.000000000E+00 0.130000000E+10 0.190000000E+10 0.230000000E+10 0.270000000E+10
0.300000000E+10 0.340000000E+10 0.360000000E+10 0.360000000E+10 0.000000000E+00

18) SLIP VALUES FOR CONCENTRATED CONNECTION
0.000000000E+00 0.000000000E+00 0.000000000E+00 0.000000000E+00 0.000000000E+00
0.000000000E+00 0.000000000E+00 0.000000000E+00 0.000000000E+00 0.000000000E+00

19) FORCES FOR CONCENTRATED CONNECTION
0.000000000E+00 0.000000000E+00 0.000000000E+00 0.000000000E+00 0.000000000E+00
0.000000000E+00 0.000000000E+00 0.000000000E+00 0.000000000E+00 0.000000000E+00

FILE FILE9: TENDON INFORMATION

```
'*****************************' /
'* INPUT FILE TEN2-12P.DAT *' /
'*****************************'/
'TITLE OF DATA FILE [FILE9]' /
'2-SPAN-SLAB L=11200, PARABOLIC TENDON' /
'CROSS-SECTION AREA [TR] (mm2)' /
652.174 /
'INITIAL STRESS IN TENDON [SIGMA(0)] ' /
1266.667 /
'# OF TENDON FIELDS [NF]' /
4 /
'TENDON GEOMETRY' /
1,29,'B',29,0,115,40 /
29,57,'E',55,0,40,200 /
57,85,'E',59,0,200,40 /
85,113,'B',113,0,40,115 /
```

INPUT FILE NOM7: INTERNAL CONSTANT VALUES

CONTROLLING CONSTANTS FOR PROGRAM DOC21

VALUE	SUBROUTINE IN WHICH CONSTANT IS USED	NAME AMD ACTION OF THE CONSTANT	
0.002000000E+03	MAIN	C1LOAD	MAX. NUMBER OF LOAD LEVEL
10	MAIN	K1MOM	MAX. # ITT. TO FIND MOMENTS
0.500000000E+03	MAIN	C1MOM	MAXIMUM ABS COMPONENT MOMENT
0.200000000E+01	MAIN	C2MOM	MAXIMUM % CHANGE OF COMP.MOMENT
20	XMOM	K1SLIP	MAX. # ITT. TO FIND SLIP
0.100000000E+04	XMOM	C1SLIP	MAX. ABS CHANGE OF INT. FORCE
0.100000000E+00	XMOM	C2SLIP	MAX. % CHANGE OF INT. FORCE
0.100000000E+01	XMOM	C3SLIP	% ALLOWED ABOVE MAXIMUM MOMENT
0.000000000E+00	XMOM	C4SLIP	(RESERVE)
5	PROP	K1PH1	MAX. # ITT. TO FIND CURVATURES
0.100000000E+03	PROP	C1PH1	MAX. ABS CHANGE OF MOMENT
0.200000000E+01	PROP	C2PH1	MAX. % CHANGE OF CURVATUE
15	PPROF	K1EIP	MAX. # ITT. TO FIND EIP
0.100000000E+03	PPROF	C1EIP	MAX. ABS CHANGE OF EIP
0.200000000E+01	PPROF	C2EIP	MAX. % CHANGE OF EIP
15	PROPS	K1EIB	MAX. # ITT. TO FILE EIB
0.100000000E+03	PSLAB	C1EIB	MAX. ABS CHANGE OF EIB
0.100000000E+02	PSLAB	C2EIB	MAX. % CHANGE OF EIB
6	MAIN	K1XM	NUMBER OF SIGNIFICANT DIGITS
0.100000000E-06	MAIN	C1XM	MINIMUM VALUE OF MOMENT
0.100000000E-06	MAIN	C2XM	MINIMUM VALUE OF SHEAR
0.100000000E-06	MAIN	C3XM	MINIMUM VALUE OF AXIAL FORCE
0.100000000E-06	MAIN	C4XM	MINIMUM VALUE OF ROTATION
0.100000000E-06	MAIN	C5XM	MINIMUM VALUE OF DISPLACEMENT
0.100000000E-06	MAIN	C6XM	MINIMUM VALUE OF SLIP
0.100000000E+03	MAIN	C7XM	MINIMUM VALUE OF EIp
0.100000000E+03	MAIN	C8XM	MINIMUM VALUE OF EAp
0.100000000E+03	MAIN	C9XM	MINIMUM VALUE OF EIb
0.100000000E+03	MAIN	C10XM	MINIMUM VALUE OF EAb

FILE NOM6:BEAM RESULTS.

LOADING # 1.00000
SPECIMEN NAME : T0: OMAPAINO + J-NNEVOIMA

TOTAL NODAL L.L. FACTORS: FORCE= .10000E+01 MOMENT= .00000E+00
Note: Total shears, moments, slips, interaction force and displacements are given at nodes.
All other values are given for elements.

----X-SECTION FORCES & MOMENTS----

SECT. #	DEFLECTION mm	SLIP mm	NODAL FORCES Force(kN)	NODAL FORCES Moment(kNm)	NODAL FORCES Total(kN)	SHEAR FORCES Slab(kN)	SHEAR FORCES Profile(kN)	MOMENTS Total(kNm)	MOMENTS Slab(kNm)	MOMENTS Profile(kNm)	AXIAL FORCES Total(kN)	AXIAL FORCES Slab(kN)	AXIAL FORCES Profile(kN)
1	0.00E+00	1.47E-11	1.85E-01	3.89E+04	-4.88E+00	-4.47E+00	-1.15E-02	3.89E+01	-1.65E+00	-4.25E-03	0.00E+00	-7.95E+02	-3.07E+01
2	1.70E-02	2.52E-12	3.70E-01	0.00E+00	-4.69E+00	-4.13E+00	-1.06E-02	3.99E+01	-7.74E-01	-1.99E-03	3.17E+02	-7.96E+02	-3.00E+01
3	3.53E-02	4.35E-13	3.70E-01	0.00E+00	-4.32E+00	-3.79E+00	-9.76E-03	4.08E+01	3.64E-02	9.37E-05	3.72E+02	-7.97E+02	-2.93E+01
4	5.41E-02	7.71E-14	3.70E-01	0.00E+00	-3.95E+00	-3.45E+00	-8.89E-03	4.16E+01	7.77E-01	2.00E-03	3.82E+02	-7.97E+02	-2.87E+01

•
•
•

----X-SECTION STRAINS & STRESSES----X-SECTION PROPERTIES----

SECT. #	STRAINS AT: SLAB/TOP SLAB/BTM	STRAINS AT: PROF./TOP PROF./BTM	STRESSES AT: MN/m2 SLAB/TOP SLAB/BTM	STRESSES AT: MN/m2 PROF./TOP PROF./BTM			CURVATURE 1/R	AXIAL STIFFNESS SLAB kN	AXIAL STIFFNESS PROFILE kN	FLEXURAL STIFFNESS SLAB kN/m2	FLEXURAL STIFFNESS PROFILE kN/m2	CENTER OF NORMAL FORCE SLAB mm	CENTER OF NORMAL FORCE PROFILE mm
1	-9.65E-05	-1.05E-04	-3.05E+00	-2.20E+01	,	,	-4.55E-08	7.84E+09	2.89E+08	3.63E+13	9.35E+10	1.22E+02	1.42E+01
,	-1.06E-04	-1.07E-04	-3.36E+00	-2.25E+01									
2	-9.92E-05	-1.03E-04	-3.14E+00	-2.17E+01	,	,	-2.13E-08	7.84E+09	2.89E+08	3.63E+13	9.35E+10	1.22E+02	1.42E+01
,	-1.04E-04	-1.04E-04	-3.28E+00	-2.19E+01									
3	-1.02E-04	-1.02E-04	-3.22E+00	-2.13E+01	,	,	1.00E-09	7.84E+09	2.89E+08	3.63E+13	9.35E+10	1.22E+02	1.42E+01
,	-1.02E-04	-1.02E-04	-3.21E+00	-2.13E+01									
4	-1.04E-04	-1.00E-04	-3.29E+00	-2.10E+01	,	,	2.14E-08	7.84E+09	2.89E+08	3.63E+13	9.35E+10	1.22E+02	1.42E+01
,	-9.94E-05	-9.91E-05	-3.14E+00	-2.08E+01									